Analysis and modeling of the effect of tides on the hydrostatic leveling system at CERN

Julien Boerez, Jacques Hinderer, Luis Rivera, Mark Jones

ANALYSIS AND MODELLING OF THE EFFECT OF TIDES ON THE HYDROSTATIC LEVELLING SYSTEMS AT CERN[1]

Julien Boerez[1, 2], Jacques Hinderer[2], Luis Rivera[2], Mark Jones[1]

[1]CERN, Geneva, Switzerland
[2]University of Strasbourg, Strasbourg, France

ABSTRACT

To meet alignment tolerances that are becoming tighter and tighter, the surveyors in the Survey Section at CERN must master the tilt effects exerted on their hydrostatic levelling system networks. These effects are many and have varied consequences, although the majority of them tilt the ground and also the water present inside HLS[2] sensors in a homogeneous way.

In order to model all inclinations together as a block, we have adjusted, at each time t, the line through the 7 sensors in the TT[3] experiment. After removal of this signal, the residual amplitudes of the readings are less than the HLS alignment tolerances of the proposed accelerator CLIC[4]. In addition, the residual signals have lost their semidiurnal and diurnal periodic components, proving that any local effects in the TT1 facility cannot be detected with the accuracy of our systems.

However, further progress has to be made to master the effect of temperature on the HLS. The periods remaining in the residual HLS signal proves the presence of un-corrected thermal effects.

Some quantitative results (numbers)

KEYWORDS: CERN, Survey, Alignment, levelling, HLS, tiltmeter, earth tides, loads

INTRODUCTION

CERN is a european organization, located on the French-Swiss border near Geneva. Starting in 1954, a number of particle accelerators have been successively built on the site. These accelerators are powerful tools for physicists trying to understand the laws governing the infinitely small.

The Survey Section at CERN is responsible for large scale metrology and alignment of accelerators and their associated beamlines. [1]

Over the generations of accelerators, the alignment tolerances imposed upon the surveyors have become tighter. For example for the CLIC project which is currently at the stage of a feasibility study, a current research objective is to meet the alignment tolerances, at 3σ, of +/- 10 microns along a 200 m moving window [2] - equivalent to a tolerance in angular measurement of +/-50 nrad. To meet such tolerances, the Survey Section has had to adapt to new technologies using very accurate alignment devices. The vertical alignment is handled by the HLS developed and distributed by Fogale Nanotech.

In the following, the system formed by the succession of magnets that form a particle accelerator will be referred to as the "machine". These magnets guide the beams formed by the particles to the experiments where the beams collide, to forward fundamental research.

---

[1] European Organization for Nuclear Research
[2] Hydrostatic Leveling System
[3] Transfer Tunnel number 1
[4] Compact Linear Collider

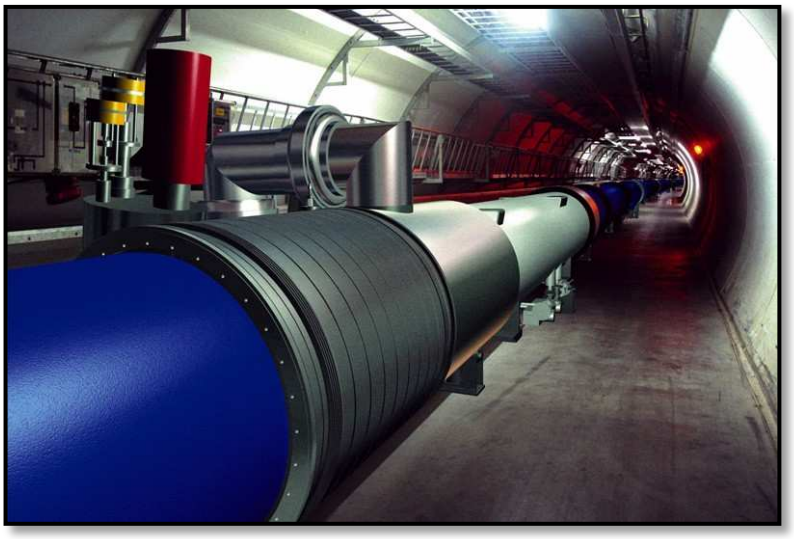

Fig.1: 3D model of the LHC magnets [5] [3]

THE HLS: VERTICAL MEASUREMENT TOOL FOR VERY HIGH PRECISION

The HLS is a system for accurate vertical measurement which doesn't need human intervention. It can work in remote irradiated areas and the sensors have a resolution of 0.2 microns, a maximum monthly deviation of 1 micron, and a measuring range of 5 mm (HLS readings start from 5 to 10 mm). A priori, an HLS can respond to the CLIC alignment tolerances.

The HLS is based on the principle of communicating vessels. In practice, a capacitive sensor is placed on a water pot. HLS pots are connected by pipes containing water. The principle of communicating vessels dictates that the water surface will have the same height (equipotential) in all the HLS pots: the water surface is the physical measuring reference of the HLS system.

Each sensor measures a capacity between two electrodes: one electrode is the sensor itself; the other electrode is the water surface. The manufacturer provides for each capacitive sensor, a polynomial calibration formula which converts the measured capacity (V) into a vertical distance (m).

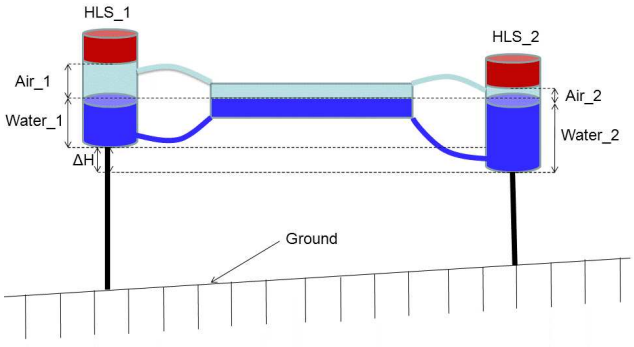

Fig.2: operating principle of the HLS

[5] Large Hadron Collider

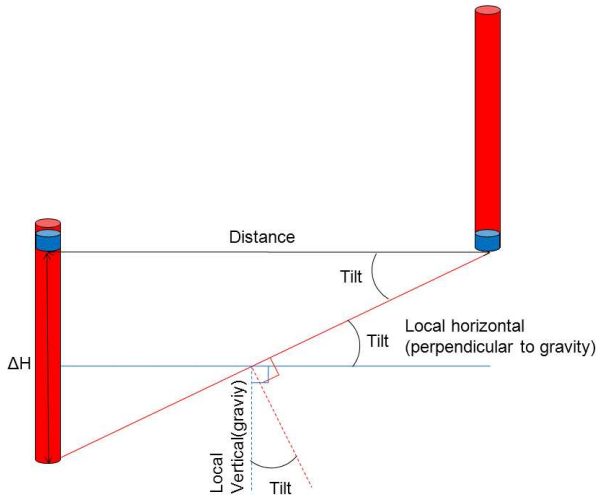

Fig.3: by design, 2 HLS also measure angles

The operating principle of a pair of HLS sensors –we will employ only the term HLS hereafter, as shown in Fig.2, allows us to measure a height difference, ΔH. The distance between two HLS is measured very precisely by standard survey instruments. From the schematic design shown in
Fig.3, we see that a pair of HLS also forms a tiltmeter. The *Tilt* angle can be determined from the following equation:

$$\text{Tilt} = \text{Atan}\left(\frac{\Delta H}{\text{Distance}}\right) \tag{1}$$

We can also derive the instantaneous angular resolution (R_T) for a pair of HLS at a given distance::

$$R_T = A\tan\left(\frac{\sqrt{\sigma_{HLS\_1}{}^2 + \sigma_{HLS\_2}{}^2}}{\text{Distance}}\right) \tag{2}$$

Where:

- σ_{HLS_n} is the a priori resolution of a HLS 0.2 µm,
- *Distance* is the horizontal distance between the two HLS.

If we consider the length of the moving window specified for CLIC: 200 m, and using equation (2), we find that we can expect a resolution of < 3 nrad at 200 m. With respect to other inclinometers described in publications, the HLS is not the most precise. By way of example the wth20 inclinometers used byNicolas d'Oreye de Lantremange in 2003 [4] had a resolution of 4.10^{-4} nrad.

TT1: EXPERIENCE AREA WITH 7 HLS IN SERIE

The TT1 is an old tunnel which was used to transfer the particles from the PS [6] to the ISR[7] which are both circular machines. In the 1980s, the ISR was dismantled, and TT1 then became a storage place for mildly radioactive cables. The interest of the TT1 is that it forms a 120 m long straight line of zero slope. Since the early 2000s, the CERN surveyors have exploited the length and stability of this tunnel to investigate as part of the CLIC feasibility studies, the tidal effects on HLS networks. [5]

Today a 140 m long HLS network (20 m along slightly sloping ground, and 120 m along flat ground), comprising 7 aligned HLS is installed in this tunnel. This experiment is very interesting because it allows us to observe the behaviour of these sensors on the same site.

All results that follow are obtained from measurements made at TT1.

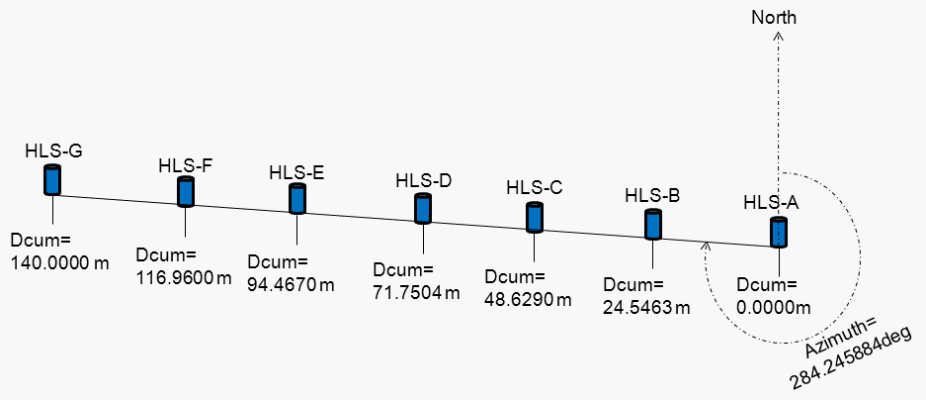

Fig.4: Outline of the HLS location at TT1 according Dcum[8]

THE EFFECTS ON HLS MEASUREMENTS

An HLS is designed to measure local ground motions which might affect the alignment of any accelerator installed on the same surface.

Let us first look at the tilt measurement formed by the vertical height difference between the 2 HLS at each end of the TT1: A and G. In comparison to the reading of just one sensor, the difference of height allows us to remove phenomena seen by both sensors such as any change in the absolute height of the water surface.

For this, let us study the tilt AG from the 14/01/2010 to the 10/02/2010, 28 days of data with a 5 min sampling rate.

[6] Proton Synchrotron
[7] Intersecting Storage Rings
[8] Cumulated Distance

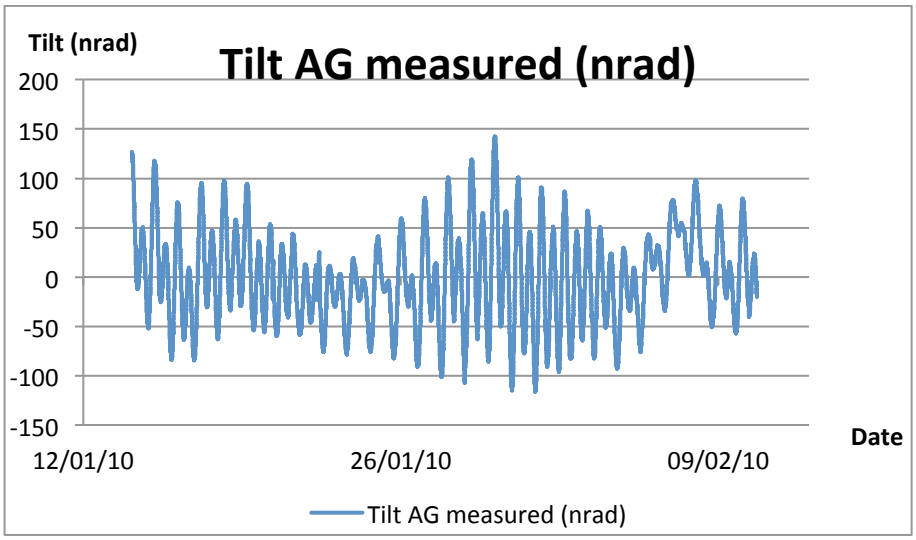

Fig.5: Measurement of the inclinometer AG from 14/01/2010 to 10/02/2010, sampling = 5 min.

The pair of HLS AG allow us to determine a tilt represented in Fig.5 in nrad. The 28 days presented show periodic phenomena. We can confirm this by performing an fft[9] on the HLS signal, the results of which are shown in Fig.6.

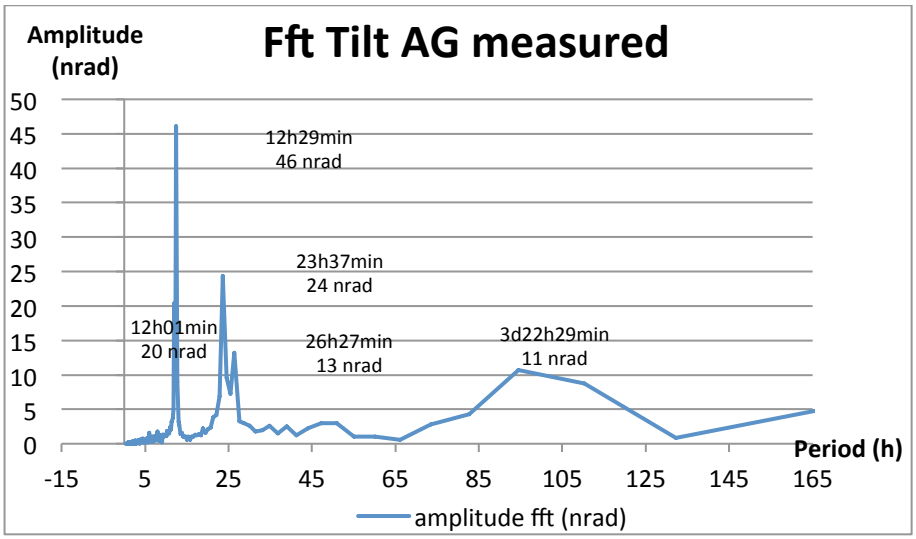

Fig.6: fft on AG Tilt measurements

The spectral representation of the HLS signal shows 5 principal periods (see Fig.6): 2 semi-diurnal waves, 2 diurnal waves and a long period wave. The time series is 662 h long, beyond 165 h, the spectrum is no longer significant.

[9] Fast Fourier Transform

Let us compare these measured periods with the catalogue of the main theoretical tidal waves.

Table 1: Characteristics of some major tidal waves caused by the Moon and Sun. [6]

symbol	origin	period
Long periods components		
Sa	S elliptic wave	365.26 j
Mm	L elliptic wave	27.55 j
Ssa	S declinational wave	182,62 j
Mf	L declinational wave	13.66 j
Diurnal components		
O1	L principal lunar wave	25 h 49 min
P1	S Solar principal wave	24 h 04 min
K1	L&S declinational wave	23 h 56 min 11s
Q1	L elliptic wave of O1	26 h 52 min
ρ1	L minor elliptic wave	24 h 51 min
Semi-diurnal components		
M2	L principal wave	12 h 25 min
S2	S principal wave	12 h 00 min
K2	L&S declinational wave	11 h 58 min
N2	L major elliptic wave of M2	12 h 39 min
L2	L minor elliptic wave of M2	12 h 11 min

If we compare Fig.6 and Table 1, $tilt_{AG}$ does actually measure the waves S2, M2, K1 and O1 which are the 4 main tidal waves. An HLS therefore measures tides, but what sort of tides?

The most famous tides are those of the oceans. The nearest celestial bodies, principally the Moon and the Sun, exert gravitational forces directly on the ocean's surface. The liquid mass of the oceans is pulled up to the celestial bodies, and then oscillates between a high and low position, dictated by the amplitude of gravitational forces.

In reality there are 3 types of tides: ocean tides, Earth tides and atmospheric tides, which are all the consequences of the gravitational forces of the nearest celestial bodies. In the case of the ocean tides the deformed surface is the ocean, in the case of Earth tides, the deformed reference system is the Earth's crust, and lastly it is the atmosphere which is deformed in the case of the atmospheric tides,.

It should also be noted that the tidal deformation has several components: potential, gravity, tilt, vertical deformation and horizontal deformation. According to the instrumentation used, one or more tidal constituents are measured. For example, a gravimeter is only subject to the variation of gravity due to the earth tides.

Returning to our situation, it is important to know which tides and what components of those tides are measured directly by the HLS. The type of tide is clearly the Earth tide since an HLS is attached to the crust through the ground. Regarding the components of the tides, an HLS is sensitive to the vertical deformation of the ground and any change in the gravity potential (observed through the instruments reference water surface which follows an equipotential of the gravity field). Both these components are commonly called a "tidal tilt". In conclusion, an HLS can measure the tilt associated with the Earth tide and its ocean loading[7].

Returning to the analysis of Fig.6 and Table 1. This data only allows us to compare the measured and theoretical periods from the tidal waves. We need to have theoretical amplitudes of local tides to compare theoretical and measured waves more rigorously. For this, we have available the *Eterna33*[10] software, which is a reference in the analysis and prediction of tides. This software was written by Hans-Georg Wenzel [8] in the 90^{s}.
Eterna33 software includes several modules. The *Predict* module, which, as its name suggests, allows us to predict the tides. For our study, we have used it to predict the tilt component of the Earth tide, at the centre of the TT1 network, along the azimuth direction of the network, over the study period, with a sampling rate of 5 min.

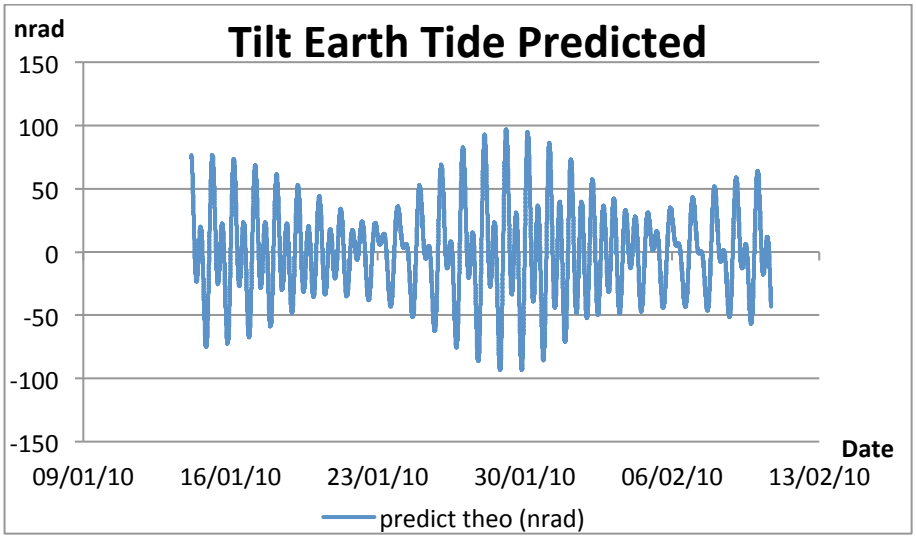

Fig.7: Predicted tide by *Eterna* at TT1

…Firstly, we see from Fig.7, which represents the theoretical Earth tide in TT1 over 28 days, that the influence of the tides is approximately + / - 100 nrad, while the CLIC alignment tolerance is + / - 50 nrad at 200 m. The magnitude of the tides is therefore 2 times higher than the alignment tolerance of CLIC.

[10] Whose version is downloadable here: http://www.eas.slu.edu/GGP/

Next, if we compare Fig.5 and Fig.7, we see that the shapes of the 2 curves are very close. This similarity is confirmed by calculation, the correlation coefficient between the measured *AG Tilt* and the Earth tide *Tilt* signal is 90%. On the other hand, the measured amplitude seems larger than the theoretical. This difference is either due to a too low an estimation of the theoretical tide and therefore a inaccurate tide model, or because other phenomena have also been measured and these should therefore be identified. To determine the cause, let us compare the spectra of the two signals.

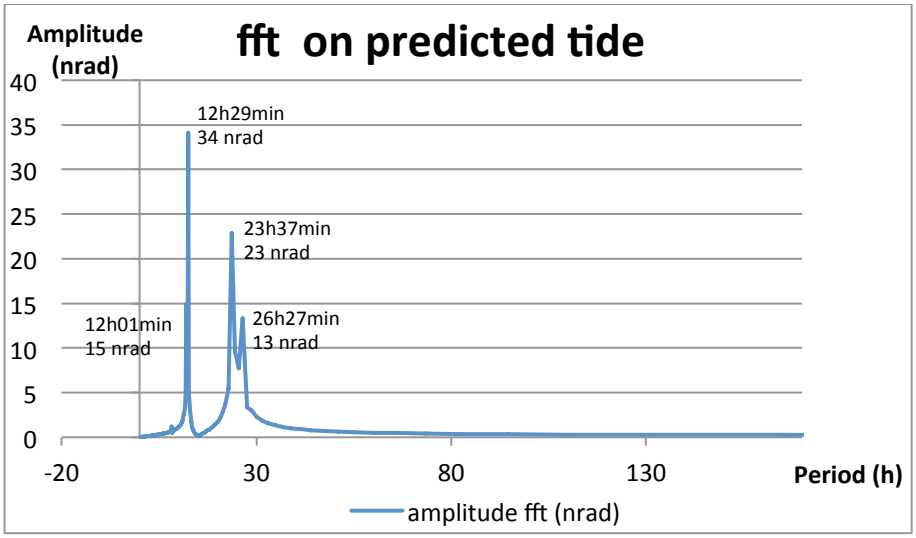

Fig.8: fft on theoretical earth tide in tilt

Fig.8 is the graphical representation of the fft carried out on the theoretical tidal signal. This graph shows the 4 principal tidal waves which can be compared to those obtained from the fft carried out on the measured signal and presented in Fig.6.

Comparison of Fig.6 and Fig.8 allows us to conclude that:

- The theoretical and measured periods are the same,
- The measured period of 3d22h29min does not appear in the theoretical model, so its cause is not the earth tides,
- The theoretical and measured amplitudes of the diurnal waves are very close,
- The theoretical amplitudes of semi-diurnal waves are lower than those measured because the model for the ocean loading has not been taken into account.

…In fact, an HLS measures predominantly the Earth tides, but also a number of other effects [9] which are all laid out in Table 2:

Table 2: Measured effects by HLS

<table>
<tr><td></td><td colspan="3">Tilt : T</td><td colspan="2">Deformation : D</td></tr>
<tr><td></td><td>Ground : T_G</td><td colspan="2">HLS : T_{HLS}</td><td>Ground : D_G</td><td>HLS : D_{HLS}</td></tr>
<tr><td rowspan="3">Periodic</td><td>Earth Tide on the ground</td><td colspan="2">Earth tide on the potential</td><td rowspan="2"></td><td rowspan="2"></td></tr>
<tr><td colspan="2">Oceanic load</td></tr>
<tr><td></td><td>Atmospheric load</td><td>Instrumental response of the water system</td><td>Local effects</td><td>Temperature</td></tr>
<tr><td>Aperiodic</td><td colspan="2">Hydrological load</td><td>Non linear effects on the ground :
- Direct effect of the geology&topography
- Direct effect from the structure</td><td></td></tr>
</table>

…The study of the effects presented in Table 2 is complicated because each one often has several consequences (simultaneous slope changes and deformations; phenomenon which are both periodic and random). Table 2 shows us this complexity, and is intended to qualify the effects according to whether they are periodic in nature or not, and according to whether they induce a tilt or a deformation either of the ground or of the instrument.
Below we detail the different effects measured by hydrostatic levelling as given in Table 2:

- The earth tide has already been described previously. It is a combination of purely periodic signals that affect both the ground and the water surface of the HLS.
- The ocean load is the indirect effect of the oscillation of the oceans that causes a global tilt of the ground. This is a purely periodic signal with tidal frequencies.
- The instrumental response of the network is the oscillation of the water system at its fundamental period, different to the tidal period, and the response time of the network coupled[11] to the measurements: the two phenomena therefore have the same periods.
- Atmospheric load is the indirect effect of the atmosphere on the crust which causes the crust to tilt. There is a component with the same period as the tides (atmospheric tides) and a random component (meteorological changes in the atmosphere).
- The hydrological load is the indirect effect of nearby water masses (lakes, groundwater) on the crust. Their effect is to tilt the ground, and its origin is generally aperiodic (weather changes).

[11] Coupled means that the response is expressed in phase with the measurements

- Local effects are the local responses of any walls or supports, the topography, and the geology to the tidal phenomena. As for the instrumental response, the heterogeneity of the walls and the environment will give a proportional response, coupled to the measures, but the effect is only local and causes a deformation (as opposed to an overall tilt). This effect is coupled to both periodic and random effects.
- The non-linear effects of the ground are all random effects that directly deform the ground locally (e.g. the sag point of a concrete gallery; ground swelling due to an underground river).
- The periodic or non-periodic temperature effects influence the instrument; the instrument support; and the ground.

There are therefore numerous effects influencing an HLS. Some of these are interdependent, and the impacts on the measurements are different. Given their relationships it is very difficult to master them independently.

Summing up the effects listed in Table 2, HLS measurements conform to the following equation:

$$M_{HLS} = T_G + T_{HLS} + D_G + D_{HLS} \quad (3)$$

Where :

- M_{HLS} is the combined tilt measurement from 2 HLS ,
- T_G is the Tilt of the ground,
- T_{HLS} is the Tilt of the water surface of HLS,
- D_G is the change in tilt caused by ground deformation,
- D_{HLS} is the change in tilt caused by deformation of the HLS and its supporting system.

CERN surveyors must realign the different machines (formed by a succession of magnets). The important question is with respect to what? For the particles to move properly through the magnets, it is important that there is no break in their path. To do this, surveyors align each machine such that the trajectory of the particles is as smooth as possible. For a large area, surveyors align the magnets progressively in a sliding window (200 m for CLIC). The important aspect of this strategy is the relative alignment within the sliding window. The beam may pass easily at time t_0, but if at time t_{+10} the surveyors must realign the machine, it is not necessary to return the magnets to their original position at t_0, the goal would be to re-align as few as possible and still deliver a smooth path for the particles.

Following this argument, a homogeneous tilt of the area in question has no influence on the relative alignment of the magnets that form the machine since the particles will still follow the same orbit. Therefore no realignment would be required.

So according to (3), the terms T_G and T_{HLS} need not be taken into account when considering any misalignment calculation for a given machine.

In the same way, the term D_{HLS} does not affect the alignment as it only affects the HLS and not the machine, it should therefore not be taken into account in any misalignment calculation.

Therefore few of the effects measured by an HLS will result in the misalignment of an accelerator. If we consider the 4 main columns of Table 2 we see that:

- A homogeneous ground tilt, T_G, would not misalign a machine because it is a long baseline phenomenon (> 200 m long).
- A uniform inclination of the surface water reference, T_{HLS}, would not misalign the machine because it is a long baseline phenomenon and it is only measured by an HLS (the ground is not affected by it).
- A heterogeneous deformation due to ground motion, D_G, could misalign the machine because it causes vertical and potentially arbitrary shifts of the ground.
- A heterogeneous deformation due to motions of HLS supports, D_{HLS}, would not create a misalignment of a machine because only the HLS is affected by it. According to Table 2, D_{HLS} is only composed by the temperature applied on the instrument.

So in conclusion we see that only the term D_G might cause a heterogeneous deformation of an accelerator and it is therefore only this component of the HLS signal which is of interest to the surveyors at CERN.

In order to master the whole collection of long baseline effects which result in a homogeneous tilt of an area, a simplified approach is going to be to model all these effects as one. To do this, one approach is to best fit a straight through the positions measured by all the HLS sensors (7 in the TT1 tunnel) at each time t_n.

The best fit line will model the global tilt, $T_G + T_{HLS}$. The residual signal (R_{LF})is given by,

$$R_{LF} = M_{HLS} - T_G - T_{HLS} \quad (4)$$

By substitution into Equation (3) we find that,

$$R_{LF} = D_G + D_{HLS} \quad (5)$$

However we want to isolate the ground deformation, D_G, from Equation (5), so we should first determine any deformation of the HLS and then carry out a least squares fit of a straight line passing through the HLS results.

Let us analyse the effect of temperature on the measured readings of the 7 HLS sensors in TT1.

Each HLS sensor is installed on a support pillar. Each support pillar is composed of different materials, with a known, measured height. The materials are anticorrosion-steel, concrete, steel, aluminium, invar, and finally the water pot of HLS. Each of these materials has an known coefficient of expansion, lying between 1 ppm[12] for invar and 22 ppm for aluminium.

To calculate the effect of temperature on each of the 7 HLS, we have the following values:

- Partial heights of the materials making up the supporting pillars (m),
- Coefficients of expansion for the materials constituting the supporting pillars (ppm),
- Temperatures measured at each of the 7 HLS (°C),
- Measured readings at each of the 7 HLS sensors(m).

Table 3: characteristics of the measured temperatures

	TEMP_A (°C)	TEMP_B (°C)	TEMP_C (°C)	TEMP_D (°C)	TEMP_E (°C)	TEMP_F (°C)	TEMP_G (°C)
Amplitude (°C)	0.34	0.40	0.32	0.78	1.18	1.68	2.43
Standard deviation (°C)	0.09	0.09	0.06	0.11	0.18	0.18	0.20

Table 3 shows us two of the principal characteristics of the temperatures measured on each of the plates supporting an HLS sensor (Temp_N is the temperature at the plate supporting HLS_N). It is clear that the spread in the temperature at a given sensor generally increases from HLS_A to HLS_G. We should note at this point that sensor G is closest to the door, so this finding is very consistent.

Table 4: characteristics of HLS measurements

	HLS_A	HLS_B	HLS_C	HLS_D	HLS_E	HLS_F	HLS_G
Amplitude (µm)	25	18	25	23	9	24	36
Standard deviation (µm)	4	3	5	3	2	5	7

If we now consider similar characteristics for the HLS measurements, we can see from Table 4 that HLS_E is very stable, whilst HLS_G has the largest spread. Contrary to the temperature readings the spread in an HLS sensors measurements is not inversely proportional to the distance from the door. In fact there does not seem to be any obvious

[12] Part per Million

relationship between the spread of HLS readings and the proximity of the door even if the values for the HLS_G sensor are the largest.

Table 5: correlation between temperatures and HLS measurements

	A	B	C	D	E	F	G
correlation betwen temperature&HLS measured (%)	42	-29	-8	-28	-20	-14	-57

Testing the correlation between the readings from the temperature and the HLS sensors, we see from Table 5, that the correlations are not constant. The coefficients can be very small (-8%) to quite high (-57%). It is also interesting to note that the correlation coefficient on A is rather strong, but opposite in sign to the other 6 coefficients.

We can however make a basic correction for the influence of temperature changes by summing the partial expansions,

$$\text{HLS\_n\_cor-temp} = \text{HLS\_n} - (\text{Temp\_n} - \text{Tref}) * \sum H\_matter * Exp\_coef \quad (6)$$

…Where,

- n is the index of the plate (A to G),
- HLS_n is the HLS measurement at point n,
- Temp_n is the temperature measured at n,
- HLS_n_cor-temp is the HLS_n measurement corrected of the temperature,
- Tref is the reference temperature (20°C)
- H_matter is the partial height of each material constituting the support,
- Exp_coef is the expansion coefficient of each material.

After correcting the HLS measurements for temperature effects in this way, we can analyse the corrected measurements, see Table 6.

Table 6: characteristics of HLS measurements after correction of the effect of the temperature

	HLS_A_cor-temp	HLS_B_cor-temp	HLS_C_cor-temp	HLS_D_cor-temp	HLS_E_cor-temp	HLS_F_cor-temp	HLS_G_cor-temp
Amplitude (µm)	24	19	25	26	21	43	47
Standard deviation (µm)	4	3	5	4	3	6	8

A comparison of Table 4 and Table 6 shows that the temperature correction degrades the quality of measurements because the amplitudes and standard deviations have increased.

The algorithm used is much too simplistic because it does not take into account the link between materials and the twist that applies during the expansion of different contiguous materials. Furthermore, no thermal inertia is calculated: the correction is made too early; and even worse: some occasional peaks in temperature are integrated by the water network giving a corrective amplitude much greater than the actual expansion.

A spectrum of temperatures shows that peaks exist at round 73h and 110h, Fig.9. We shall return to these values later.

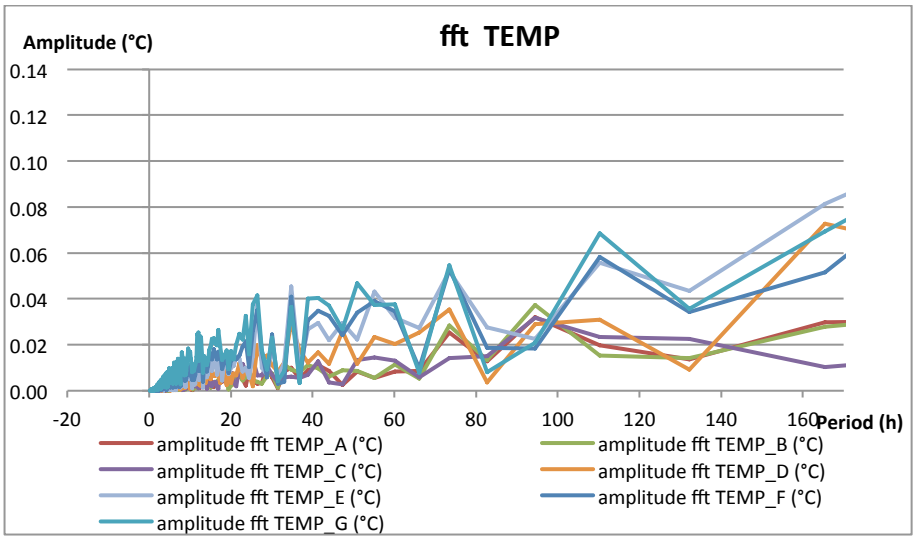

Fig.9: fft of measuring temperatures

The study of the effect of temperature changes on HLS readings is not trivial. Further in-depth studies by finite element analysis for example, would better control this effect because the correlation coefficients in Table 5 show that there is sometimes a causal link between temperature variations and HLS measurements.

Taking into account the effects of temperature variations with the correction algorithms available degrades the measurements, we have therefore taken the decision to not apply any correction. In ignoring the effect of temperature changes on the HLS, there will remain in the residuals after any other processing, a sign affecting only the HLS which would not give rise to any misalignment of an accelerator. The study of the effect of temperature on the measurements HLS remains open to future research in order to improve the corrective model.

Let us now consider the linear fit to the measurements from the 7 HLS.

STUDY OF THE 7 HLS MEASUREMENTS PRESENT AT TT1

If we consider that the temperature effects, D_{HLS}, remain part of the HLS measurements, M_{HLS}, then Equation (5) reduces to:

$$D_G = R_{LF} \tag{7}$$

The method proposed above to reach this equality is, at each time t, to calculate the best straight line through the 7 HLS readings using a least squares algorithm.

Let us consider the same time series as before: from 14/01/2010 to 10/02/2010 i.e. 28 days of data, with a 5 min sampling rate; and look at the behaviour of the 7 sensors behaviour before any processing. The measured readings from the 7 HLS sensors are presented for this time series in Fig.10.

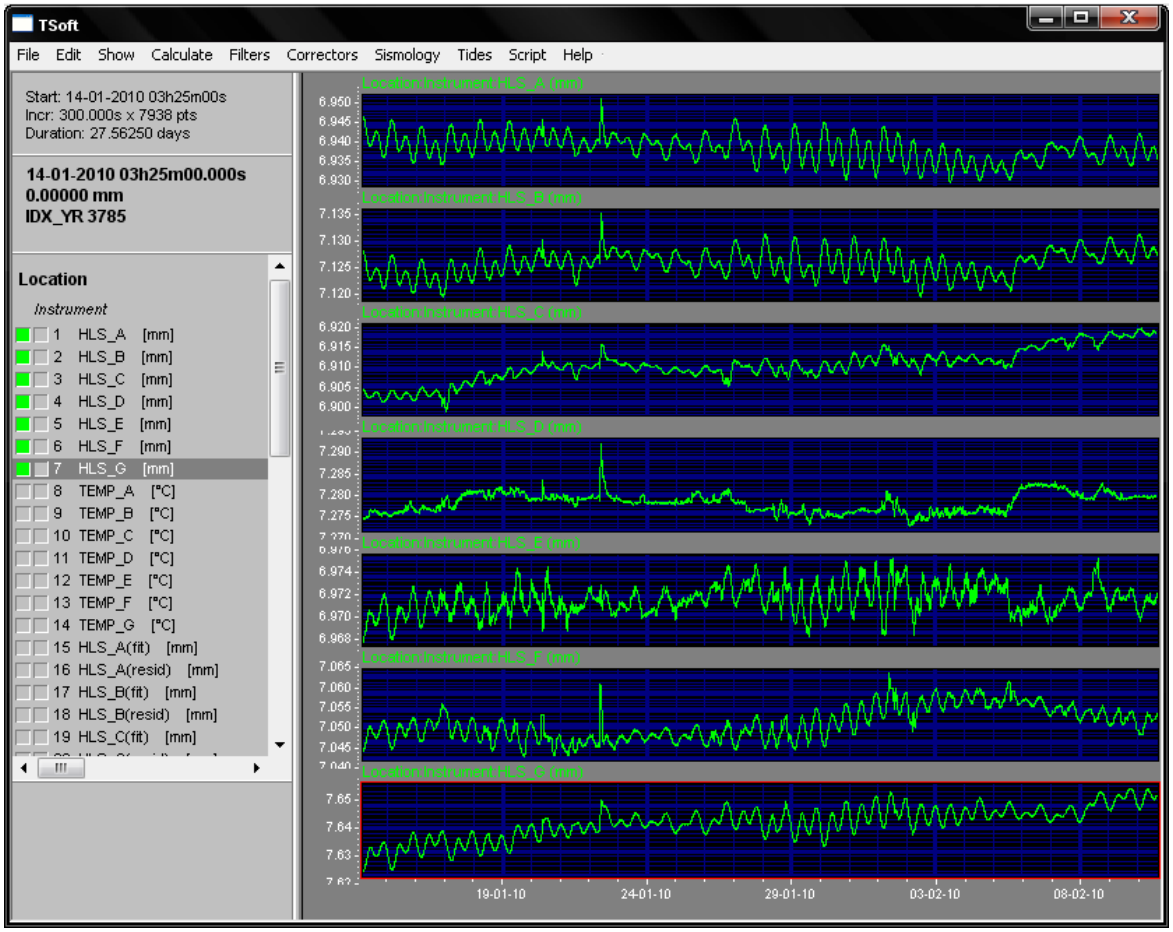

Fig.10: 7 HLS raw readings

The signal is in millimetres, the units of the data capture software.

We can see that the sensor readings are not centred around a common value, instead they lie between 6.900 mm and 7.650 mm. This "important" range is due to the site installation, each sensor is not installed at exactly the same altitude.

It is also evident that the readings have some periodic behaviour, and that the further the sensor is from the centre of the hydrostatic system, the stronger and clearer the periodic phenomenon is. This finding is due to long baseline tilt phenomena on the network. As there is a conservation of the water volume between two moments in time, the whole network tilts around the pivot point at the centre of the network. As we move away from this centre, the inclination will be greater and the signal/noise ratio better, giving a cleaner signal.

Before adjusting the measurements, we must re-centre them around a common value. To achieve this, let us set the zero value at the centre of the time series at a time which *Eterna33* predicts a null tide (27/01/2010 10:25 p.m.).

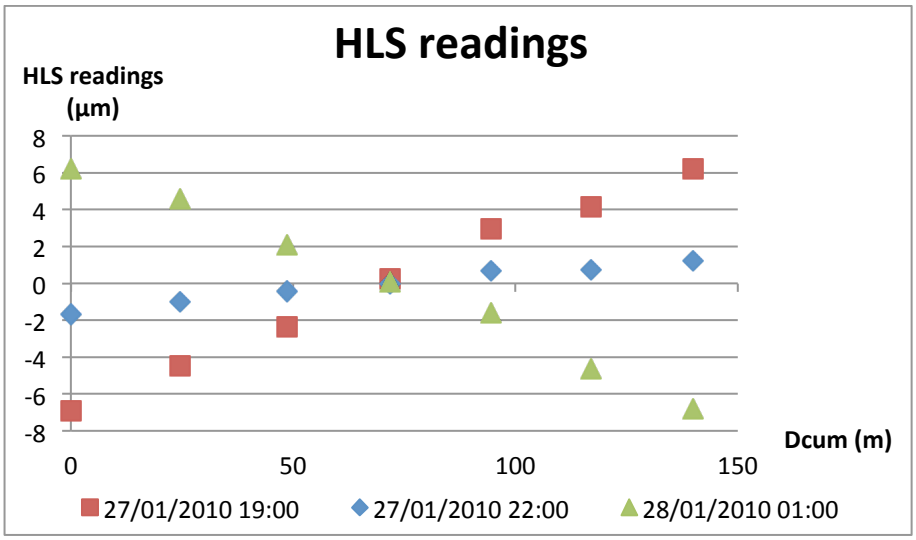

Fig.11: HLS readings according to Dcum, t_0 = 27/01/2010 10:25 pm

In Fig.11 are show three sets of HLS sensor readings, all re-centered with respect to t_0, and as a function of the cumulative distance along the HLS installation.

We see that the HLS readings follow a straight line representing the overall inclination of the area. It is therefore reasonable to pass a straight line (see Equation (8)) through the 7 points.

$$\hat{H}(n)=a.DCUM(n)+b+v(n) \quad (8)$$

Where:

- $\hat{H}(n)$= adjusted HLS(n) readings at time t,
- a=slope of the adjusted straight line at time t,
- b=intercept of the adjusted straight line at time t,
- v(n)=residue of HLS(n) at time t.

The HLS sensor has a resolution of 0.2 µm, and a maximum monthly drift of 1.0 µm. The adjustment will depend on the accuracy of the sensor, and also on the deformation of the network. The a priori accuracy, σ_0, of a HLS with respect to the best fit line will therefore represent at the same time the sensor accuracy, a part of the drift of the sensor, and a share of local, non-linear deformation. Let us set σ_0 to 1 µm and apply it to all the diagonal terms of the weight matrix, because all the sensors should have the same accuracy. At each time t, let us calculate with *Matlab* the best fit line by the method of least squares. It must be noted that the redundancy is not very high, we have 7 observations to determine the two unknowns, a and b, of Equation (8).

After the adjustment, we get an a posterior value of 1.8 µm for σ_0, which represents the quality of the least squares fit. This value is very satisfactory and represents both the precision of the HLS and the stability of the TT1 tunnel.

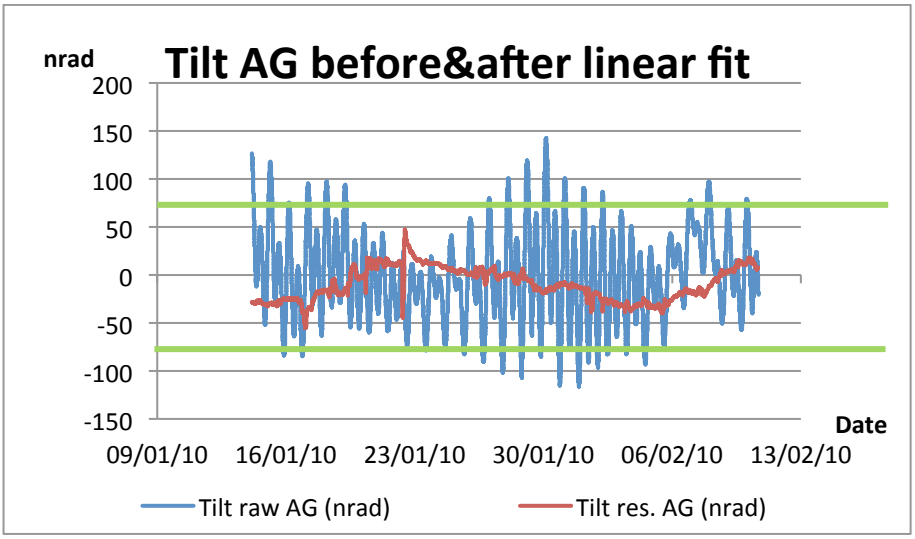

Fig.12: AG Tilt before and after linear fitting

If we apply the corrections determined using this method to the tilt measured between the sensors at each end of the HLS network we can see the results inFig.12. The horizontal bars represent the angular projection of the CLIC alignment tolerance (+/- 10 micrometres) at 140 m. The residuals are there well inside the CLIC alignment tolerances.

Table 7: summary of HLS values before and after linear fitting

	Raw HLS	Adjusted HLS	HLS residues
Standard deviation HLS_A (µm)	4	4	1
Standard deviation HLS_B (µm)	3	3	1
Standard deviation HLS_C (µm)	2	2	1
Standard deviation HLS_D (µm)	3	1	2
Standard deviation HLS_E (µm)	1	2	1
Standard deviation HLS_F (µm)	4	2	3
Standard deviation HLS_G (µm)	4	3	2
Amplitude HLS_A on the series (µm)	23	21	5
Amplitude HLS_B on the series (µm)	19	19	3
Amplitude HLS_C on the series (µm)	17	16	9
Amplitude HLS_D on the series (µm)	24	15	11
Amplitude HLS_E on the series (µm)	8	16	13
Amplitude HLS_F on the series (µm)	22	19	18
Amplitude HLS_G on the series (µm)	25	22	12

If we compare the amplitudes and standard deviations of the measured HLS signal before and after the correction, see Table 7, we see that the standard deviations after the adjustment between the 7 sensors are of the same order of magnitude (between 1 and 3 micrometres). This means that the sensors all have the same accuracy and that the

deformations at the points where they are installed are of the same order of magnitude. The adjusted sensor's amplitudes were higher on the sensors at the ends of the network in comparison with central ones because the distance from the centre is higher and therefore the amplitude of the sensor is greater: the lever arm principle.

The magnitudes of the residuals suggest that the sensor readings from HLS_D to HLS_G are more dispersed. This finding should be assessed with the reality on field. HLS_G is closest to the door and it is subject to the greatest temperature variations due to the opening of the door. As we approach HLS_A, this thermal effect will decrease and the measurements become more stable.

From the results presented in Fig.12 we can also see that the residual tilt AG after correcting with the best fit straight line, is much more stable than before correction.

Let us now look at the residuals for the 7 HLS, Fig.13, in greater detail.

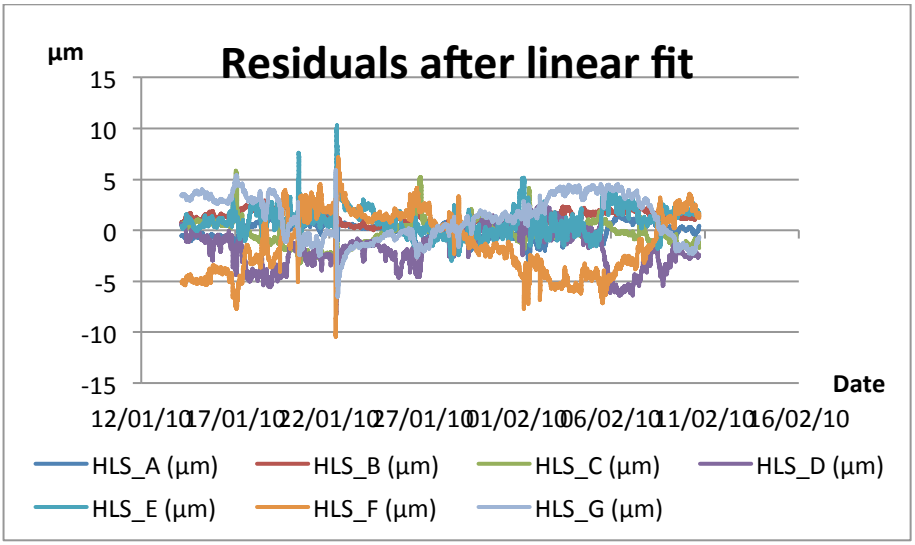

Fig.13:7 HLS residues after linear fit

The results shown are those sought by the surveyors: local movements of the ground filtered out from the long base tidal and other loading effects (ignoring any thermal influences).

All have the same order of magnitude: between +/-7 µm except for a peak-point on 23/01/2010. The accuracy of 7 HLS sensors when carrying out the least squares adjustment have the same order of magnitude, indicating that all the HLS measure comparable phenomena and none suffer from instrumental problems. Finally, the spectra, Fig.14, shows that no sensor has any significant residual (several times greater than the noise) in the semi-diurnal and diurnal periods. Therefore the differences in the local effects at TT1 are weaker than the accuracy of the HLS.

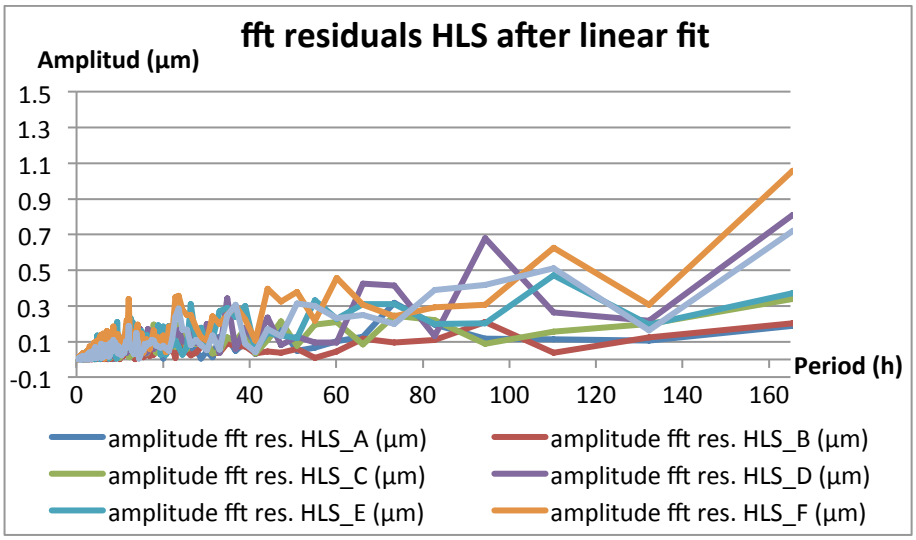

Fig.14 : fft on HLS residues after linear fit

The residuals at tidal periods are negligible: less than 0.4 µm according to Fig.14. The highest values are at 73, 94, and 110 hours. These figures should be compared to the periods identified in the temperature variations which were presented inFig.9, and they therefore prove the presence of temperature effects in the residuals.

CONCLUSIONS

The 3σ pre-alignment tolerance for CLIC is +/-10 microns in a sliding window of 200 m. To meet this tolerance the survey team can use HLSs for vertical alignment.

The sensor specifications meet the surveyors needs. However an HLS measures other effects than the local deformations of the ground that could misalign the machine.

To meet the requirements of the CLIC, it is necessary to filter the undesirable effects from the HLS measurements. To do this, the modelling of these long base effects thanks to the 7 TT1 HLS has given satisfactory results, thereby allowing HLS to meet the alignment requirements of CLIC. However, this model could be improved by correctly modelling the effect of temperature on the HLS and its supports.

Finally, the 7 aligned HLS along TT1 form a research experiment, but we do not, for existing accelerators, meet such a useful situation very often, where so many sensors along a long, straight line. We will therefore have to propose an alternative corrective method for the long base effects, which will be viable for a network of just 2 or 3 sensors.

ACKNOWLEDGEMENTS

It is primarily thanks to Bernard Ducarme from ICET and his welcome advice that this subject thesis was born. He directed the principal author to the University of Strasbourg and more specifically to Jacques Hinderer and Luis Rivera to supervise the thesis. Thank you to Sophie Lambotte, Séverine Rosat, Laurent Longuevergne, Jean-Paul Boy who have guided me, advised me and provided both models and data.

Another thank you goes to the CERN, without which the need for this research wouldn't exist, and to Mark Jones for his advice and his availability for approaching 3 years. Finally, thank you to my colleagues Michael Betz, Sébastien Guillaume, Sylvain Griffet and Thomas Touzé for their technical advice and reviews.

References

1. **SU.** SU : large scale metrology. *SU : large scale metrology.* [Online] CERN. [Cited: 01 01 2011.] https://espace.cern.ch/be-dep-ABP-SU/.

2. **Touzé, Thomas.** *Proposition d'une méthode d'alignement de l'accélérateur linéaire CLIC.* Geneva, Switzerland : s.n., 2010. Thesis report. P2-P33.

3. **CERN.** LHC machine outreach. *CERN.ch.* [Online] CERN. [Cited: 04 01 2011.] http://lhc-machine-outreach.web.cern.ch/lhc-machine-outreach/images/dipole-in-tunnel-graphic.jpg.

4. **LANTREMANGE, Nicolas d'OREYE de.** *INCLINOMÈTRE À NIVEAUX HYDROSTATIQUES DE HAUTE RÉSOLUTION EN GÉOPHYSIQUE.* Louvain La Neuve, Belgium : s.n., 2003. Thesis report. P158.

5. **Thomas, Touzé.** *Proposition d'une méthode d'alignement de l'accélérateur linéaire du CLIC.* Geneva, Switzerland : s.n., 2011. Thesis report. P120.

6. **Lambotte, Sophie.** *Vibrations propres basse fréquence et déformation de marée. Impact des hétérogénéités locales et contribution à l'étude de la source des grands séismes.* Strasbourg, France : s.n., 2007. Thesis report. P14.

7. **Paul, Melchior.** *THE EARTH TIDES.* [ed.] Permagon Press. Brussels : Pergamon Press, 1966. P123-P126.

8. **Wolfgang, Torge.** Wenzel. *Angewandte Geophysik Jena.* [Online] 2000. http://www.geo.uni-jena.de/geophysik/etc/wenzel.html.

9. **Longuevergne, Laurent.** *Contribution à l'hydrogéologie.* Paris, France : s.n., 2008. Thesis report. P35-P42.